ISSN 2347-3487

Effect of rapid solidification and calcium additions on Sn-38 wt.%Pb-6 wt.%Sb melt-spun alloys

Rizk Mostafa Shalaby[1,*], Shalabia Badr[2], Nermin Ali Abdelhakim[1] and Mustafa Kamal[1]
[1] Metal Physics Laboratory, Physics Department, Faculty of Science, Mansoura University, Mansoura, Egypt, P. O. Box: 35516.
[2] Physics Department, Faculty of Science, Mansoura University, Mansoura, Egypt
*Corresponding author: doctorrizk2@yahoo.co.uk

Abstract

The effect of calcium additions on the structure and physical properties of melt-spun process Sn-38Pb-6Sb alloys have been experimentally investigated at a solidification rate of ~10^5 K/s. Structure, internal friction, elastic moduli, microhardness and electrical resistivity of the Sn-38%Pb , Sn-38%Pb -6%Sb , Sn-38%Pb -6%Sb-0.5%Ca , Sn-38%Pb -6%Sb -1%Ca , Sn-38%Pb -6%Sb -1.5%Ca , Sn-38%Pb -6%Sb -2%Ca , Sn-38%Pb -6%Sb -2.5%Ca (in wt%) rapidly solidified alloys are investigated. The results showed that the mechanical and electrical properties values are enhanced for ternary Sn-38%Pb -6%Sb alloy. The examined mechanical and electrical conductivity decreased by addition of calcium content in the studied alloys. It also leads to with increasing Ca content the SnSb inter-metallic compound (IMC) precipitates are increased in the Sn matrix. The results were explained in terms of the dislocation theory, effect of quenching rate on the produced density fluctuations in composition and the modes of interaction of crystal lattice defects.

Keywords

Melt-spun process; mechanical properties; electrical resistivity; micro-hardness.

Council for Innovative Research
Peer Review Research Publishing System
Journal: JOURNAL OF ADVANCES IN PHYSICS
Vol. 11, No. 4
www.cirjap.com, japeditor@gmail.com

ISSN 2347-3487

1. Introduction

We intend to complete previous work by Kamal et al [1]. The high cooling rate in the melt-spinning technique makes the time necessary for diffusion insufficient to yield a solid alloy that is homogeneous in composition. In other words, solidification under non equilibrium conditions will yield an alloy with composition far from uniform [1]. The process of rapid solidification leads to the formation of amorphous and fine microstructures [3], new intermediate phases [4] and anomalous vacancy concentrations [5]. In Pb-Sn alloys directionally solidified in a positive thermal gradient, marco-segregation along the length of the sample takes place [6]. Pb-Sn eutectic alloy was reported to show outstanding super plasticity [7]. The addition of antimony to the solder Pb-Sn alloys gives the way to have a higher strength and lower plasticity compared to the lead-tin alloys. Some investigations show that addition of other elements such as silver or copper in certain industrial applications at certain level may be useful to produce alloys with desirable properties. It was suggested that alloying additions may interface with nucleation event by changing the precipitate characteristics and/or boundary properties [8]. The nucleation and growth of the solid during solidification of Pb and Pb-Sn alloys were examined by electrical resistivity [9]. In failure mode analysis of tin–lead solders in electronics, it is often observed that a decrease in solder joint strength is closely related to microstructure changes. Upon solidification of eutectic solder 63Sn37Pb, a two-phase microstructure is developed, the morphology of which is dependent upon the rate of solidification [10]. The microstructure changes at room temperature and it includes precipitation of tin colonies within the lead-rich phase as well as an overall coarsening of lead-rich particles contained within the tin-rich matrix. A decrease in the strength of the solder is observed with these microstructural changes [11], thereby counteracting improvements in the mechanical strength realized through the finer morphology generated by faster cooling rates. The mechanical properties of many low melting alloys change gradually with time at room temperature because of minute changes in structure. This aging at room temperature is sometimes referred to as room temperature recrystallization or annealing. Aging sometimes has the effect of increasing the hardness and strength of the alloy, but it can also have the opposite effect. For example, a chill-cast quaternary eutectic of tin, bismuth, cadmium, and lead shows an increase in strength of about 34% after 16 weeks of aging at room temperature [12]. Lead-antimony alloys exhibit the same age-hardening property. If heated above their solid solubility temperature and then quenched, they show a marked increase in hardness on aging, the extent of which is dependent on the amount of antimony present and the rate of cooling [13]. The present work aims to reveal some properties of adding Ca to the ternary melt spun process of Sn-Pb-Sb alloys used for electro-winning circuit. These series of alloys will be subjected to electrical and mechanical studies. Especially the mechanical studies will focus on properties such as internal friction, elastic moduli and microhardness.

2. Experimental techniques

A. Alloy design and preparation

In the present work, lead alloys were prepared from high purity elements (99.99%). The calcium content added to the tin base ternary Sn-38wt.%Pb-6 wt.%Sb alloy. The components were melted in an electric furnace at 800 K. Some of the samples were prepared as ribbons by using the single roller type melt spinning technique, reported by Kamal et al. [2, 14, 15]. Melt spun ribbons were between 40 and 120 μm thick and 6 mm wide. The Solidification front velocity in the ribbons was estimated to be 30.4 m s^{-1}.

B. Structure, mechanical and electrical properties measurements

X-ray diffraction (XRD) analysis is carried out with a X-ray diffractometer (XRD, X′ pert PRO, PANalytical using CuKα target with secondary monochromator, in Central Metallurgical R and D institute, Technical Service Department, El-Tebbin, Helwan, Cairo) was used to identify the structure of all produced alloys. The internal friction and the dynamic Young's modulus measurements were carried out with a modified dynamic resonance vibrator which vibrates electro-dynamically [14]. Hardness measurements were conducted on both the rapidly solidified samples by using microhardness tester, [Model FM.7 Future Tech. Corp. Tokyo Japan]. A load of 10 gm was applied for 5 s as indentation time, and the VHN was given automatically by the system. Electrical resistivity measurements for the tested samples were made by using the Kelvin Double-Bridge method in the temperature range from 290 to 380 K. The variation of temperature during the resistance - temperature investigation, was carried out by using a step-down transformer connected to a constructed temperature controller. The heating rate was kept constant during the investigation at 5 K min^{-1}.

3. Results and discussions

3.1. X-ray diffraction analysis

Fig. 1 shows the produces x-ray diffraction pattern of Sn-38%Pb , Sn-38%Pb -6%Sb , Sn-38%Pb -6%Sb-0.5%Ca , Sn-38%Pb -6%Sb -1%Ca , Sn-38%Pb -6%Sb -1.5%Ca , Sn-38%Pb -6%Sb -2%Ca , Sn-38%Pb -6%Sb -2.5%Ca (in wt%) rapidly quenched from melt by melt spun process, the pattern shows the existence of three kinds of phases ,Pb-phase with face centered cubic structure, Sn-phase with tetragonal structure and antimony tin phase with rhombohedral (hex.) structure and appearance of SnSb intermetallic compound (IMC) increases with increasing calcium addition. The calculated lattice parameter for β-Sn is indicated in Table (1).

ISSN 2347-3487

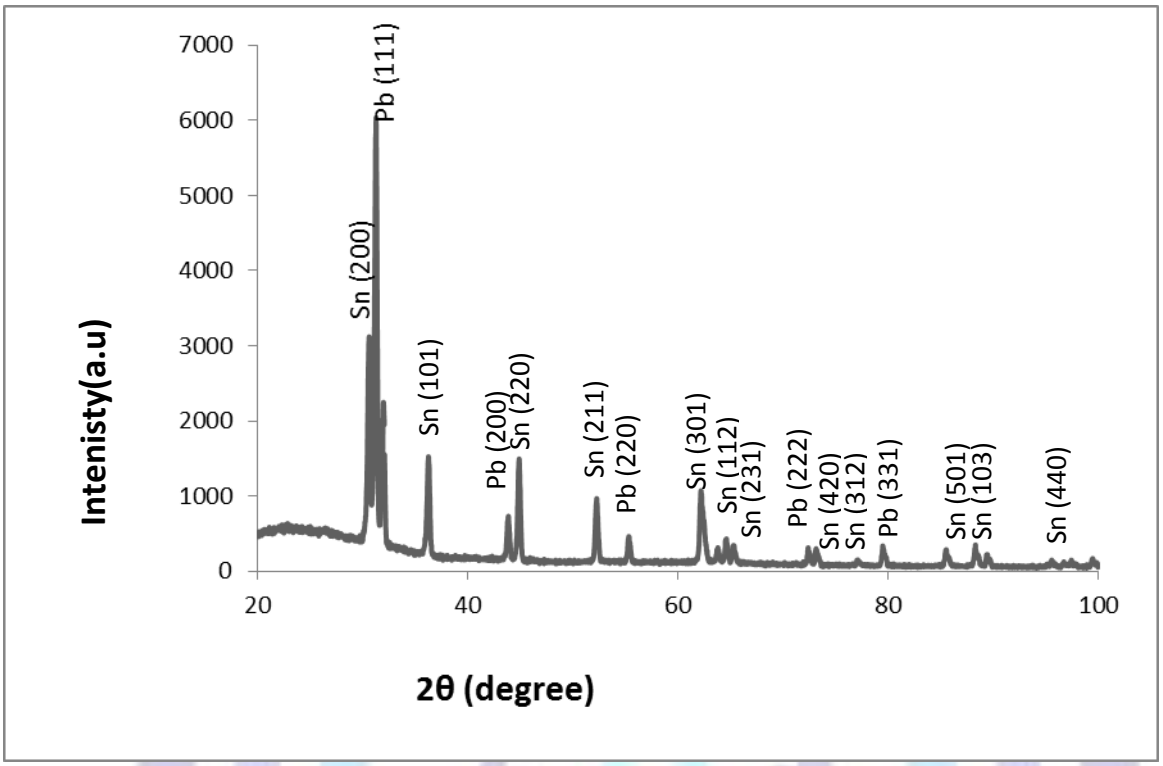

Figure (1.a) X-ray diffraction pattern of Sn-38%Pb melt spun alloy

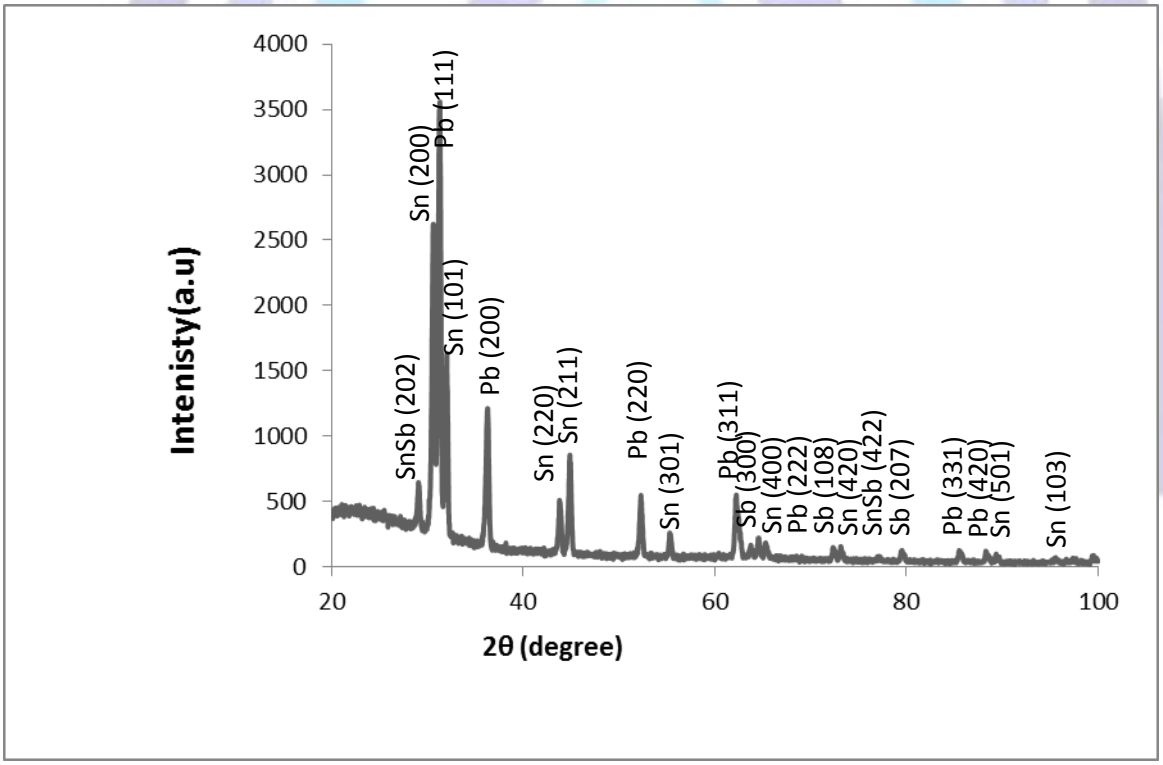

Figure(1.b) X-ray diffraction pattern of Sn-38%Pb-6%Sb melt spun ribbon

ISSN 2347-3487

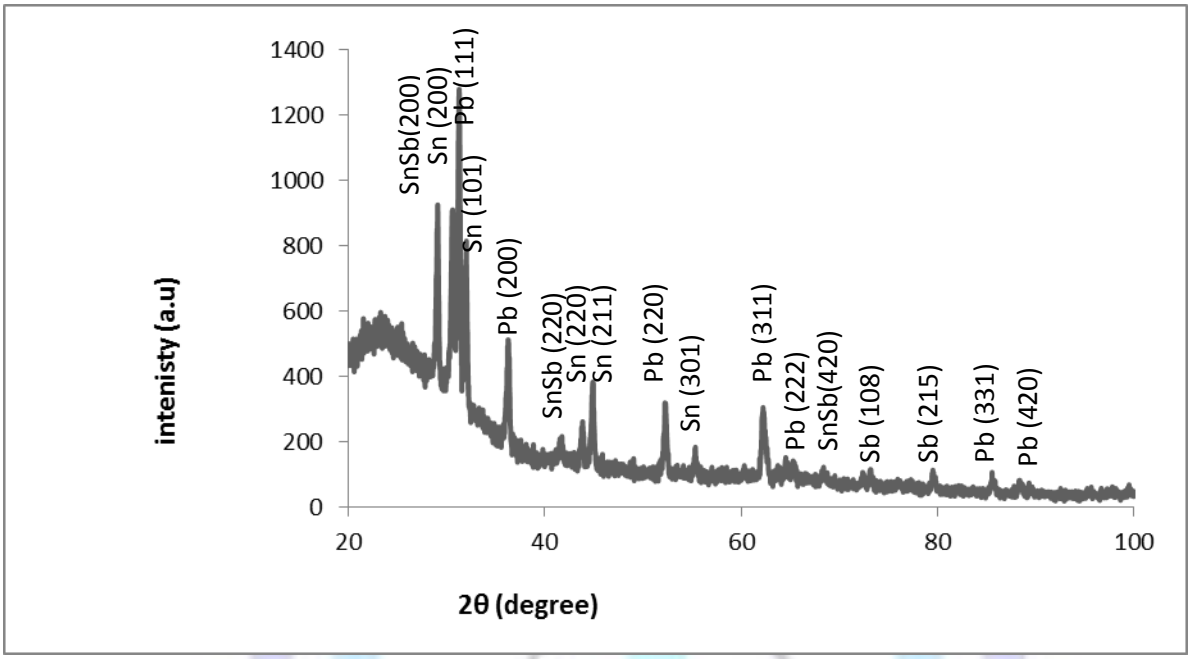

Figure (1.c) X-ray diffraction pattern of Sn-38%Pb-6%Sb-0.5%Camelt spun ribbon

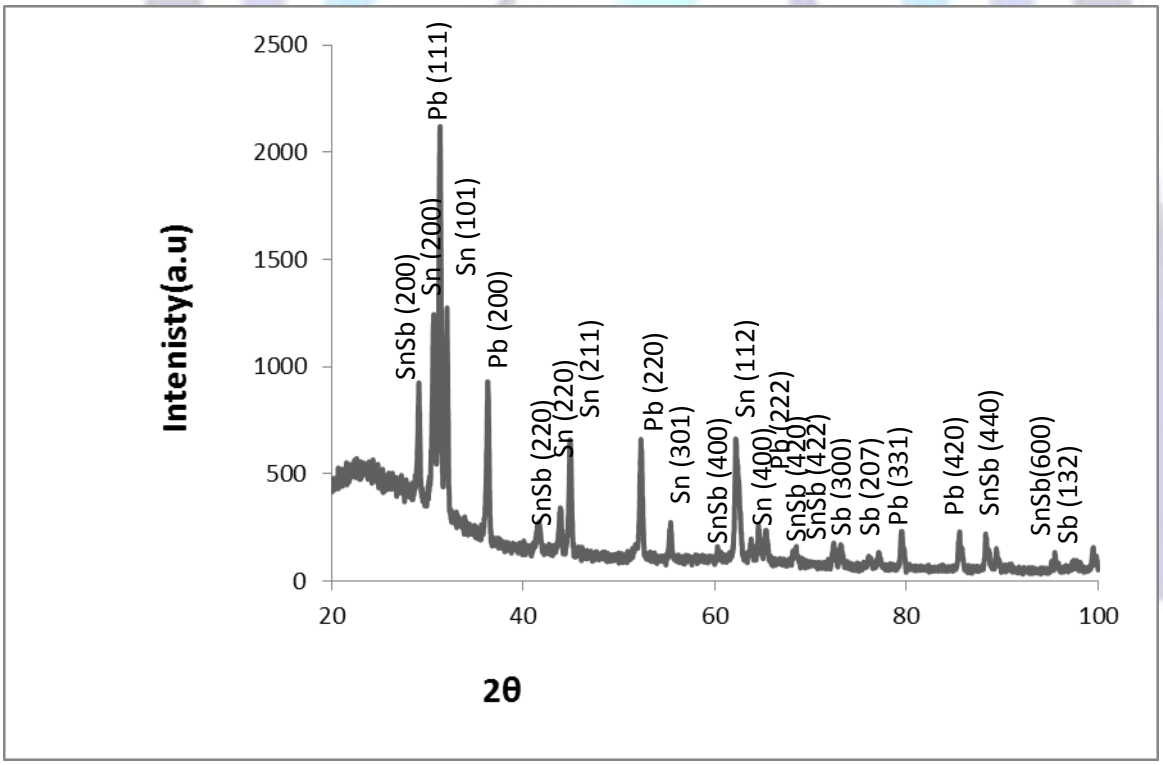

Figure (1.d) X-ray diffraction pattern of Sn-38%Pb-6%Sb-1%Camelt spun ribbon

ISSN 2347-3487

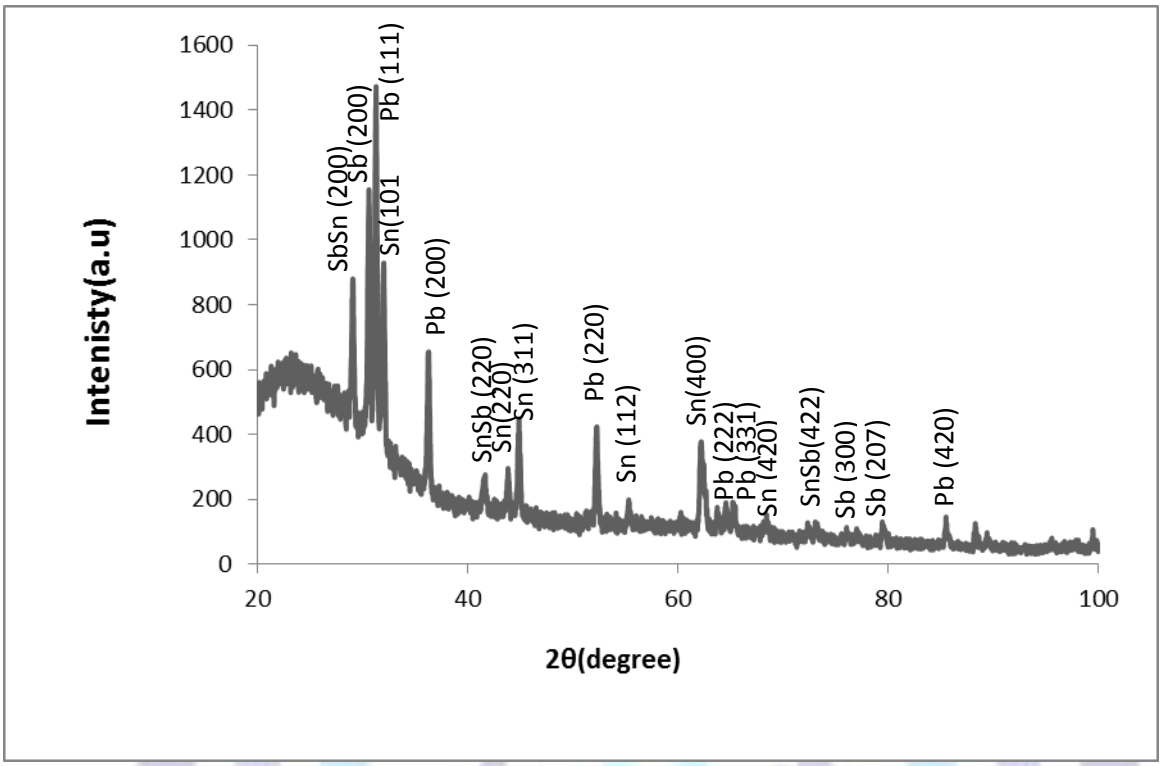

Figure (1.e) X-ray diffraction pattern of Sn-38%Pb-6%Sb-1.5%Camelt spun ribbon

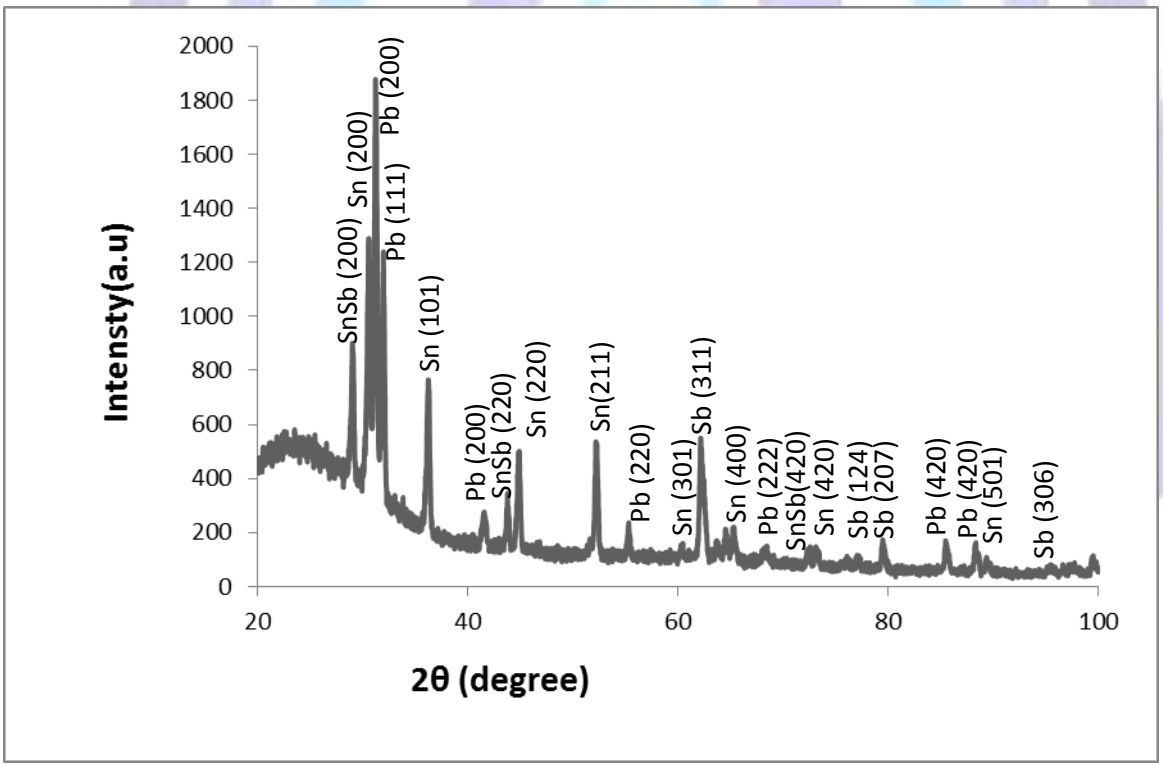

Figure (1.f) X-ray diffraction pattern of Sn-38%Pb-6%Sb-2%Ca melt spun ribbon

ISSN 2347-3487

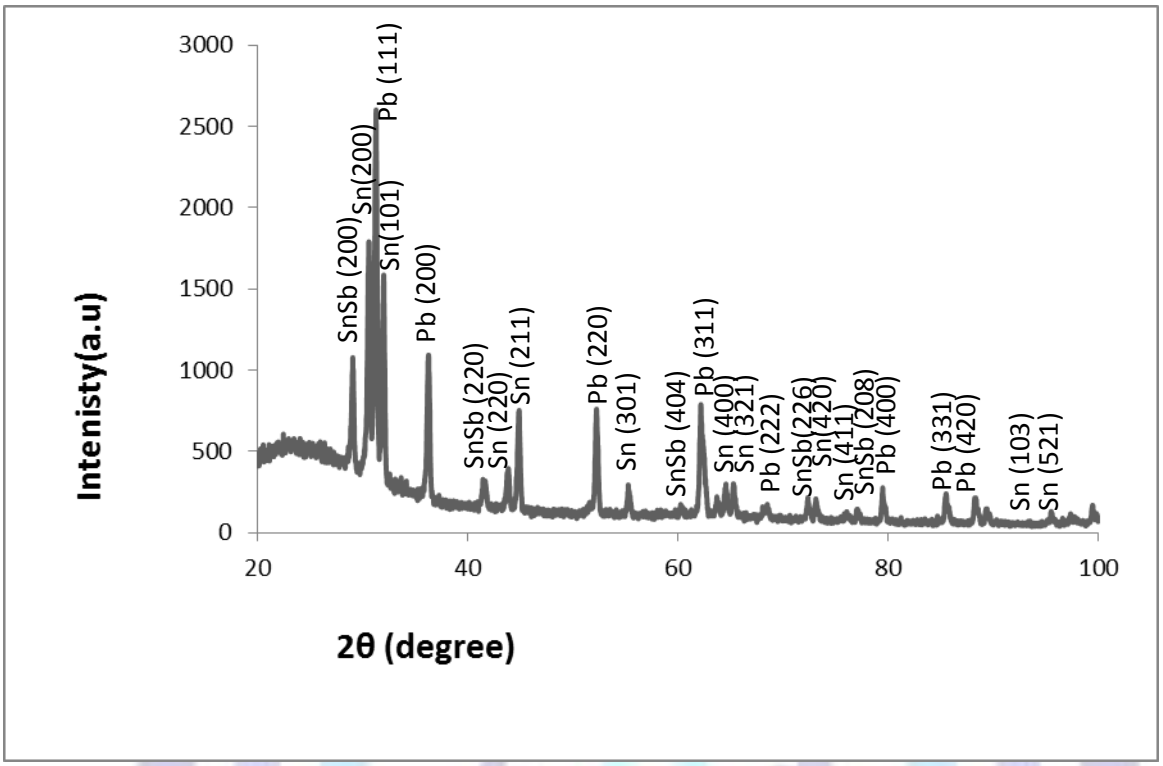

Figure (1.g) X-ray diffraction pattern of Sn-38%Pb-6%Sb-2.5%Camelt spun ribbon

Table 1: Lattice parameter of β-Sn for all melt spun ribbons

System	a (Å)
Sn-38%Pb	5.843
Sn-38%Pb-6%Sb	5.842
Sn-38%Pb-6%Sb-0.5%Ca	5.852
Sn-38%Pb-6%Sb-1%Ca	5.848
Sn-38%Pb-6%Sb-1.5%Ca	5.849
Sn-38%Pb-6%Sb-2%Ca	5.843
Sn-38%Pb-6%Sb-2.5%Ca	5.841

The number of atoms per unit cell in any metal crystal is partially dependent on its Bravais lattice. The number of atoms per cell in a face centered lattice must be a multiple of 4. Turning to the crystal structure of compounds of unlike atoms, it is find that the structure is built on the skeleton of a Bravais lattice, but that certain other rules must be obeyed, precisely because these are unlike atoms present [16]. So the next step is to find the number of atoms per unit cell in lead –phase in the melt spun-ribbons. To find this number we use the following equation $\rho = \frac{1.6602 \sum A}{V}$, where ρ =density (gm/cm^3), $\sum A$=sum of the atomic weights of the atoms in the unit cell and V is the volume of the unit cell (Å^3). From above equation we have ∑A=ρV/1.6602 and ∑A = nM, Where n is the number of atoms per unit cell, A is the molecular weight. When determined in this way, the number of atoms per cell is always an integer, within experimental error. In our experimental work the melt spun ribbons of Sn-38%Pb , Sn-38%Pb -6%Sb , Sn-38%Pb -6%Sb-0.5%Ca , Sn-38%Pb -6%Sb -1%Ca , Sn-38%Pb -6%Sb -1.5%Ca , Sn-38%Pb -6%Sb -2%Ca , Sn-38%Pb -6%Sb -2.5%Ca(in wt%) as indicated in the table 2 , atoms are simply missing from a certain fraction of those lattice sites which they would be expected to occupy , and the result is a non integral number of atoms per cell.

ISSN 2347-3487

Table 2: Number of atoms per unit cell for all melt-spun ribbons

System	n (no of atoms/unit cell)
Pb-5wt%sn	3.685
Pb-5wt%Sn-2wt%Sb	2.958
Pb-5wt%Sn-2wt%Sb-0.5wt%Ca	2.860
Pb-5wt%Sn-2wt%Sb-1wt%Ca	3.700
Pb-5wt%Sn-2wt%Sb-1.5wt%Ca	2.820
Pb-5wt%Sn-2wt%Sb-2wt%Ca	3.11
Pb-5wt%Sn-2wt%Sb-2.5wt%Ca	3.56

3.2. The electrical properties of quenched ribbons:

Electrical resistivity is usually used in measuring the electrical conductivity of the alloys, and as a physical property of an electronic packaging material, it also attracted more and more researchers attention. Anything which increases the frequency of collisions of electrons with ions raises the resistivity, thermal vibration, foreign atoms in solid solution, and plastic deformation of the lattice lower the conductivity. Thus itis found in this study that the electrical resistivity of the studied melt-spun alloys increase with rise in temperature as indicated in figures(3)for , Sn-38%Pb -6%Sb-0.5%Ca , Sn-38%Pb -6%Sb -1%Ca , Sn-38%Pb -6%Sb -1.5%Ca , Sn-38%Pb -6%Sb -2%Ca , Sn-38%Pb -6%Sb -2.5%Ca (in wt%).

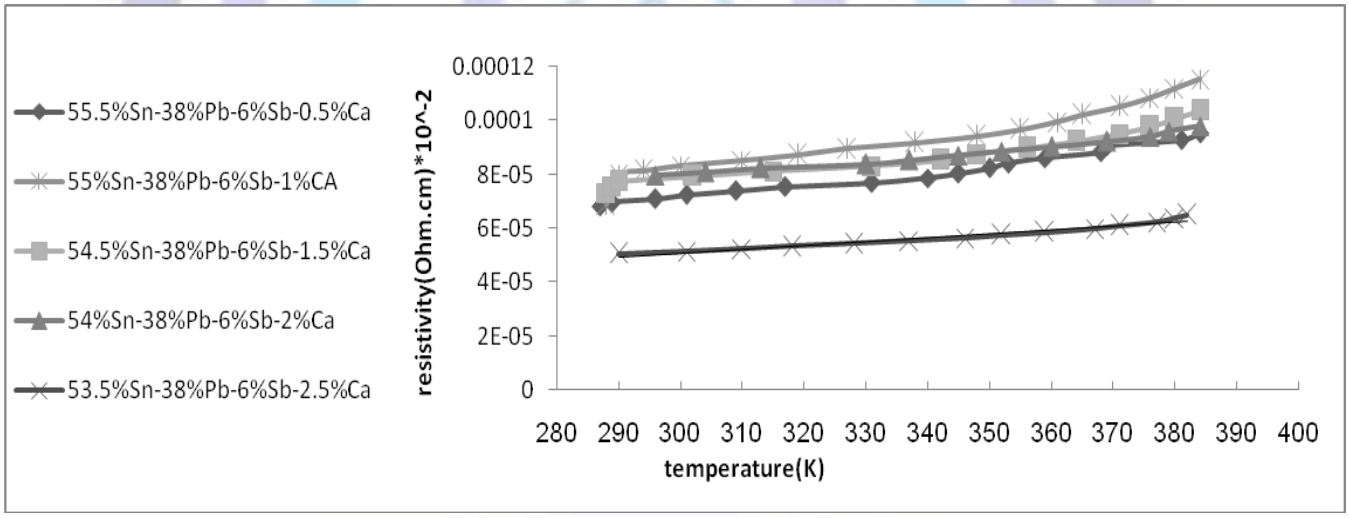

Fig.3: Electrical resistivity versus temperature for all melt spun ribbons

The distortions produced by alloying elements are independent of the temperature. Their effects are additive to the effect of thermal vibration. At higher temperatures the thermal disturbance of the lattice can be described in terms of quantized elastic waves or phonons, and the increase in electrical resistivity can be visualized resulting from collisions between electrons and phonons. The resistivity here is measured around room temperature so that the total resistivity pronounced minima at composition of 2wt%Ca.This correspond to the formation of ordered alloys. Moreover, by addition of Ca to Sn-Pb-Sb solid solution formation causes a pronounced decrease of electrical resistivity. In multiphase alloys the electrical conductivity tends to change proportionally with composition between the electrical conductivity of the phases. Factors affecting the collision processes or as it is usually called the problem of scattering ,such as static imperfections, lattice vibrations, magnetic ions or by scattering by more than one mechanism operate at the same time, all reduce the electrical conductivity of a metallic alloy , because these imperfections mean that there are irregularities in the electrical fields within a metal. Irregularities reduce the mobility of an electron and finally the electrical conductivities [17]. Electrical conductivities values are tabulated in table 3.

ISSN 2347-3487

Table 3: Electrical conductivity for all melt spun ribbons

System	σ $(\Omega\ m)^{-1}$
Sn-38wt%Pb	0.72
Sn-38wt%Pb-6wt%Sb	2.11
Sn-38wt%Pb-6wt%Sb-0.5wt%Ca	1.46
Sn-38wt%Pb-6wt%Sb-1wt%Ca	1.45
Sn-38wt%Pb-6wt%Sb-1.5wt%Ca	1.37
Sn-38wt%Pb-6wt%Sb-2wt%Ca	1.3
Sn-38wt%Pb-6wt%Sb-2.5wt%Ca	1.98

3.3. Heat conductivity

The thermal conductivity changes in approximately the same way as was developed for electrical conductivity of metals. Whereas both processes are due to electron transport they rely on different aspects, namely flow of charge and flow of energy .However, whereas in pure metals the heat conductivity was related to the electrical conductivity by the well-known Widemann-Franz law [18-20] is given by

$\frac{k}{\sigma t} = l = 2.45 \times 10^{-8} V^2 k^{-2}$. The constant l is termed Lorenz number, and k is the thermal conductivity. In metallic alloys the changes in electrical conductivity with composition do not follows the changes in electrical conductivity according to this ratio, the changes being in the same direction but to a different degree. Some investigations [21] have shown that there is a definite relationship between the electrical and thermal conductivity of metallic alloys, although the Wiedeman-Franz ratio doesn't hold .The relationship for thermal conductivity is that K (thermal conductivity) = 5.02 σT x 10^{-9} + 0.03 , where T; is the absolute temperature. A tabulation of the Pb-Sn-Sb-Ca melt spun ribbons with their thermal conductivities is shown in table (4).

Table 4: Thermal conductivity for all melt spun ribbons

System	K $(wm^{-1}k^{-1})$
Sn-38wt%Pb	1.12
Sn-38wt%Pb-6wt%Sb	3.13
Sn-38wt%Pb-6wt%Sb-0.5wt%Ca	2.2
Sn-38wt%Pb-6wt%Sb-1wt%Ca	2.2
Sn-38wt%Pb-6wt%Sb-1.5wt%Ca	2.1
Sn-38wt%Pb-6wt%Sb-2wt%Ca	1.8
Sn-38wt%Pb-6wt%Sb-2.5wt%Ca	2.9

3.4. Thermal diffusivity

Using dynamic resonance technique and from the frequency $f_{0,\,at}$ which peak damping occurs, the thermal diffusivity D_{th} can be obtained from the $D_{th}=2t^2f_0/\pi$, where t, is the thickness of the melt-spun ribbon. For Sn-Pb-Sb-2wt%Ca quenched ribbons, the thermal diffusivity is smaller than the other compositions as shown in table 5. Thermal diffusivity D_{th} is transport coefficient which is related to microscopic transport of heat. A nonlinear decrease of thermal diffusivities with an increase in calcium content is observed in all quenched ribbons.

ISSN 2347-3487

Table 5: Thermal diffusivity for all melt spun ribbons

System	$D_{th}(m^2.sec^{-1}) \times 10^{-8}$
Sn-38%Pb	9.54
Sn-38wt%Pb-6wt%Sb	13.6
Sn-38wt%Pb-6wt%Sb-0.5wt%Ca	11.6
Sn-38wt%Pb-6wt%Sb-1wt%Ca	4.62
Sn-38wt%Pb-6wt%Sb-1.5wt%Ca	4.2
Sn-38wt%Pb-6wt%Sb-2wt%Ca	0.95
Sn-38wt%Pb-6wt%Sb-2.5wt%Ca	3.3

We assume this fact is caused by smaller aggregation of calcium particles. The aggregates could improve the heat transport and improve thermal diffusivity. The value of thermal diffusivity of quenched ribbons controls the time rate of temperature change as heat passes through quenched ribbons. So it is a measure of the rate at which a body with a non-uniform temperature reaches a state of thermal equilibrium. The mathematical formula that relates thermal conductivity (k) and temperature-dependent specific heat at constant pressure (heat capacity) is $D_{th} = \frac{K}{C_p \ \rho}$, where ρ is the temperature-dependent density and C_p is the temperature-dependent specific heat at constant pressure [22], so that by knowing the value of thermal conductivity as indicated in table (4), the specific heat C_p can be calculated as indicates in the following table (6).

Table 6: Specific heat for all melt spun ribbons

System	$C_p(j.k^{-1}.kg^{-1}) \times 10^4$
Sn-38%Pb	0.174
Sn-38wt%Pb-6wt%Sb	0.37
Sn-38wt%Pb-6wt%Sb-0.5wt%Ca	0.198
Sn-38wt%Pb-6wt%Sb-1wt%Ca	0.65
Sn-38wt%Pb-6wt%Sb-1.5wt%Ca	0.8
Sn-38wt%Pb-6wt%Sb-2wt%Ca	3.4
Sn-38wt%Pb-6wt%Sb-2.5wt%Ca	1.8

3.5. Mechanical behavior for all quenched ribbons

3.5.1. Internal friction

The internal friction of the Pb-Sn-Sb-Ca melt spun ribbons is an important characteristics which are indirectly related to their elastic properties .Solid objects have a characteristic of mechanical resonant frequencies (f) which are related to the ribbons mass, dimension, and elastic properties. The vibration analyzed from the internal friction point of view (r), i.e., the dissipation of vibration energy in the ribbon sample, or damping mechanical loss. Q^{-1} deduced from the amplitude decay a free vibration as shown in table 7. In general, the hysteretic rearrangement of microstructural features upon application of a dynamic load causes internal friction. So the internal friction measurements have been quit beneficial and productive for learning about the behavior of Sn-Pb-Sb-Ca quenched ribbons, where the internal friction is able to respond to small changes in the mechanical state of quenched ribbons. It is found that the anelastic component (the time-dependent elastic behavior) is small and negligible.

Table 7: Internal friction for all melt spun ribbons

System	Q^{-1}
Sn-38%Pb	0.088
Sn-38wt%Pb-6wt%Sb	0.081
Sn-38wt%Pb-6wt%Sb-0.5wt%Ca	0.096
Sn-38wt%Pb-6wt%Sb-1wt%Ca	0.134
Sn-38wt%Pb-6wt%Sb-1.5wt%Ca	0.113
Sn-38wt%Pb-6wt%Sb-2wt%Ca	0.164
Sn-38wt%Pb-6wt%Sb-2.5wt%Ca	0.116

3.5.2 Elastic moduli

Young`s modulus is one of the important characteristics that reflect strongly the interaction and the bonding nature among constituent atoms [23]. The elastic constants of the metallic alloys which were fundamental physical properties especially for the mechanical properties such as strength, plastic deformation and fracture were reported previously using single crystals [24]. A number of researchers have given the empirical relationships to relate shear modulus (G), bulk modulus and the young's modulus (E) for various elements [25, 26]. Poisson's ratio, defined as the lateral contraction per unit breadth divided the longitudinal extension per unit length in simple tension, is reported to provide more information about the character of the bonding forces than any other elastic coefficients [27, 28].Poisson ratio (v) is related to young's modulus (E), shear modulus (G) and bulk modulus by equations G = E/2(1+v). Figure (4) shows resonance curves for Sn-38%Pb -6%Sb-0.5%Ca , Sn-38%Pb -6%Sb -1%Ca , Sn-38%Pb -6%Sb -1.5%Ca , Sn-38%Pb -6%Sb -2%Ca , Sn-38%Pb -6%Sb -2.5%Ca (in wt%)melt spun alloys .

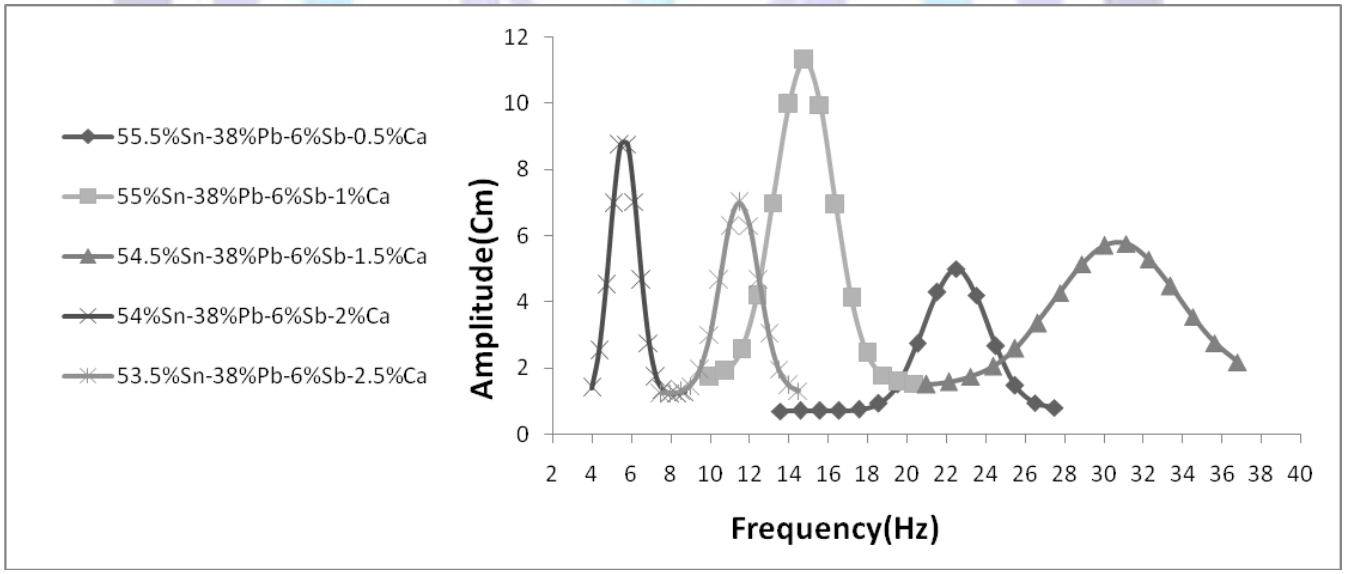

Fig.4: Resonance curves for all melt-spun ribbons

The magnitude of elastic constants defect-free metal alloys is only a function of the magnitude of the stiffness of the atomic bonds. In real polycrystalline melt-spun alloys, other factors such as porosity, concentration of impurities, intergranular phases and alloying elements may influence the magnitude of the elastic constants. The nominal elastic modulus value for Sn and its alloys commonly is taken as 50 GPa but experimental values collected from literature for pure tin and its alloys can vary between 16 55 GPa [29].The reasons for this wide variation in experimental value of elastic modulus have been investigated in this study. The calculating values of young`s modulus (E) using dynamic resonance method of rapidly solidified alloy were studied. Values of elastic modulus E, bulk modulus B and shear modulus G are listed in table 8.

Table 8: Elastic moduli for all melt spun ribbons

System	E (GPa)	G (GPa)	B (GPa)	G/E
Sn-38%Pb	16.5	5.95	25.1	0.36
Sn-38wt%Pb-6wt%Sb	60.9	22	87.3	0.361
Sn-38wt%Pb-6wt%Sb-0.5wt%Ca	29.4	10.6	42.1	0.36
Sn-38wt%Pb-6wt%Sb-1wt%Ca	15.6	5.65	22.3	0.362
Sn-38wt%Pb-6wt%Sb-1.5wt%Ca	12.5	4.5	17.8	0.36
Sn-38wt%Pb-6wt%Sb-2wt%Ca	4.3	1.56	6.14	0.363
Sn-38wt%Pb-6wt%Sb-2.5wt%Ca	7.5	2.6	16.7	0.35

Clearly changing the calcium content leads to a marked decreasing in mechanical properties of Sn-Pb-Sb quenched ribbons .One may conclude, the calcium content has a profound influence on the strength and stiffness of these quenched ribbons from melt. It is also observed that in most quenched ribbons, that are in all composition G is about 0.35 E.

3.5.3. Hardness

It is obvious from the table (9) that the apparent hardness values dependent on calcium addition for all quenched ribbons. The value of H_v is found to vary from 116 MPa to 178 MPa. But this variation is not linear in behavior. This type of nonlinear behavior, it is known as indentation size effects (ISE). The ISE behavior can be explained qualitatively on the basis of penetration depth of indenter [30, 31]. The increase of hardness number can be attributed to solid solution hardening mechanism and refinement the crystalline size by addition of indium and cooling rate.

Table 9: Vickers hardness for all melt spun ribbons

System	Hv (MPa)
Sn-38%Pb	116.0
Sn-38wt%Pb-6wt%Sb	161.8
Sn-38wt%Pb-6wt%Sb-0.5wt%Ca	127.0
Sn-38wt%Pb-6wt%Sb-1wt%Ca	167.0
Sn-38wt%Pb-6wt%Sb-1.5wt%Ca	133.0
Sn-38wt%Pb-6wt%Sb-2wt%Ca	147.4
Sn-38wt%Pb-6wt%Sb-2.5wt%Ca	178.0

Conclusions

Based on the experimental results of structural and physical analysis of quenched ribbons, the following conclusions can be drawn:

1- It was conclude that the resistivity pronounced minima at composition of Pb-5wt% Sn-6wt%Sb. This also corresponds to the formation of ordered quenched ribbons.

2- For ternary alloy containing antimony, Sn-38wt.%Pb-6wt.%Sb alloy it noticed that increase the electrical conductivity, thermal conductivity, thermal diffusivity and mechanical properties.

3- We noticed that, calcium addition to ternary alloy minimize the thermal diffusivity, thermal conductivity, elastic modulus, electrical conductivity except the Vickers hardness increase to maximum value at 2.5 wt.% Ca.

4- We recommend that ternary Sn-38wt.%Pb-6wt.%Sb alloy more suitable for electro-winning circuits and engineering applications.

References

[1] Mustafa Kamal, Shalabia Badr and Nermin Ali Abdelhakim, International Journal of Engineering & Technology IJET-IJENS Vol:14 No:01

[2] M. Kamal, J.C. Pieri and R. Jouty, Mém. Sci. Rev. Mét., Mars, 143 (1983).

[3] N.R. Green, J.A. Charles, G.C. Smith, Mater. Sci. Technol. (UK) 10, 11, 977 (1994).

[4]Q.Li, E. Johnson, A. Johansen and L. Sarhoft-Kristensen, J. Mater. Res. 7, 2756 (1992).

[5] G. Thomas and R.H. Willens, Acta metall., 13, 139 (1965), and 14, 138 (1966).

[6] S.N. Tewari, and R.Shah, Metall. Trans. A, Phys. Metall. Mater.Sci. (USA) 23A (12), 3383 (1992).

[7]P.Zhang, Q.P.Kong and H.Zhou, Phil. Mag. A. Phys. Condens. Matter.Struct.Defects Mech. Prop.(UK) 77 (2), 437 (1998).

[8]I.Manna and S.K. Pabi, phys. stat. sol. (a), 123, 393 (1991).

[9] S. H. Liu, D. R. Poilier and P. N. Ocansey, Metall. Mater. Trans. A, Phys. Metall. Mater.Sci., 26 A (3), 741 (1995).

[10] P. T. Vianco and D. R. Frear, “Issues in the Replacement of Lead-Bearing Solders,” Journal of Materials, pp. 14–18 (July 1993).

[11] R. J. Klein Wassink, Soldering in Electronics, 2nd ed., Electrochemical Publications Ltd, Scotland, 1989, pp. 141–147.

[12]Manko, H. H., Solders and Soldering,McGraw-Hill, (1964).

[13] Holmes, J. F., "Lead and Its Alloys,"Metal Industry, Vol. 8, (December 1961).

[14] M. Kamal, A. M. Shaban, M. El-Kady and R. Shalaby, Radiation Effects and Defects in Solids, 138, 307 (1996).

[15] M.Kamal, A.M.Shaban, M.El-Kady and R.M.Shalaby, 2nd International Conference of Engineering Physics and Mathematics, Faculty of Engineering, Cairo University, Cairo, Vol.2,pp.107-121,1994.

[16] B. D. Cullity ,Elements of X-ray diffraction, Addison-Wesley Series Metallurgy and Materials ,(1956), Ch.2 .

[17] Mustafa Kamal and Abu- Bakr El-Bedewi, Journal of Material Science .Materials in Electronics 11, (2000) 519-523.

[18] G. Wiedemann ,R.Franz ,Ann.Phys .89, 497 (1853) .

[19] A. Sommerfeld ,NaturWissenschaften 15,825 (1927).

[20] Makariy A. Tanatar ,JohnpierrePaglione , CedomirPetrovic ,Louis Taillefer ,Science , June (2007) Vol.316 , PP:1320-1322 .

[21] G. E. Doan, The Principles of Physical Metallurgy, McGraw-Hill Book Company, Inc. 52-743 (1953) PP: 215-217.

[22] J. E. Parrott and Audrey D. Stukes , Thermal Conductivity of Solids , (1975)Pion Limited ,ISBNO 85086 047 4 PP:1-11 .

[23] A. Inoue, H. S. Chen. J. T. Krause, T. Msumoto, M. Hagiwara, Journal of Materials Science, 18, 2743-2751 (1983).

[24] Morihiko Nakamura and kazuhiro Kimura, Journal of materials Science 26,

2208-2214 (1991).

[25] H. M. Ledbetter, Mater. Sci. Eng., 27,133 (1977).

[26] T. Gorecki, Mater. Sci. Eng., 43,225-230 (1980).

[27] Anish Kumar, T. Jayakumar, Baldev Raj, K. K. Ray, ActaMaterialia 51, 2417-

2426 (2003).

[28] W. Koster and H. Franz, Metall. Rev; 6(21):1(1961).

[29] CemalBasaran, Jianbin Jiang, Mechanics of Materials, 34, 349-362 (2002).

[30] U.Kolemen ,O. Uzun ,M. Ydmazhar, N. Gülclü, Y. Yanmaz , Journal of Alloys and Compounds, 415(2006) 300-306 .

[31] K. Sangwal ,B.Surowska , Mater .Res. Innov. 7 (2003) 91-104 .